Modeling and Control of a Pneumatically Driven Stewart Platform

Hubert Gattringer, Ronald Naderer and Hartmut Bremer

Abstract Electrically driven Stewart platforms are used in the field of machine tooling and robotics, where very accurate positions have to be reached associated with heavy loads. In this paper we present a pneumatically driven Stewart platform powered by fluidic air muscles. Due to the elasticity of the muscles and air as driving medium, the robot is predestined for applications where compliance plays a major role. Compliant behavior is necessary for direct contact with humans. Fitness is an area, where this contact is given and a fast movement is needed for the body workout. Another field of application are simulators for computer games or 6D cinemas. To realize the six degrees of freedom $(x, y, z, \alpha, \beta, \gamma)$ for the Tool Center Point (TCP) there are six fluidic muscles. Due to the fact that the muscles are only able to pull on the platform, there is a spring in the middle that applies a compressive force to the moving part of the robot. The spring is a non modified spiral spring which is commonly used for the suspension of a passenger car. As a result of the kinematical model (inverse kinematics, forward kinematics) the workspace is optimized. To dimension and test the dynamical behavior, a Matlab/Simulink model is derived. This is done by applying the Projection Equation, a synthetical method for obtaining the equations of motions for multi body systems. Based on the dynamical model we develop a control concept in a cascaded structure (pressure control, linearization, position control). A laboratory setup is used to validate the simulation model. Both, simulations as well as experimental results demonstrate the success of the proposed concept.

Hubert Gattringer
Institute for Robotics, Johannes Kepler University Linz, Altenbergerstr. 69, 4040 Linz, Austria;
E-mail: hubert.gattringer@jku.at

Ronald Naderer
FerRobotics Compliant Robot Technology GmbH, Hochofenstr. 2, 4030 Linz, Austria,
E-mail: ronald.naderer@ferrobotics.at

Hartmut Bremer
Institute for Robotics, Johannes Kepler University Linz, Altenbergerstr. 69, 4040 Linz, Austria;
E-mail: hartmut.bremer@jku.at

H. Ulbrich and L. Ginzinger (eds.), Motion and Vibration Control, 93–102.

1 Introduction

In modern life, manufacturing companies without robotic systems are hard to imagine. Normally these are articulated robots for manipulation tasks and Hexapod systems in milling machines. In [12] and [13] a hexapod system is introduced using stiff electrical drives with a very high accuracy. Some basics for parallel kinematic robots can be found in [8, 9].

For applications where humans are directly involved, like fitness devices or simulators for virtual environments, compliance plays a major role. The compliance can be reached by using pneumatic muscles as driving units instead of stiff electric servo drives. In this paper we present a parallel kinematic built as a Stewart platform with a movable upper platform and a fixed lower platform connected by six fluidic muscles, see [14] for details. The muscles can only pull on the platform, so a pre-stressed spring in the middle of the hexapod delivers the compressive forces. Figure 1 shows the design of the system under consideration. To move the platform in the 3D space some kinematical calculations are done. The inverse kinematical problem is easily evaluated by vector chains, while the forward kinematics is solved numerically. The Projection Equation [2] is used to derive a dynamical model of the hexapod. By inserting the trajectories with their time derivatives, the inverse dynamical model can be used to improve the behavior in the sense of a feed forward control. The feedback control is realized as cascaded structure consisting of a pressure control, linearization of the muscle behavior and a linear position control, see [4]. Some basic concepts for controlling fluid muscles can be found in [10]. Singh et al. [16] show the design and control of a single pneumatic actuator that also acts against a pre-stressed spring. An enhancement of the valve-actuator behavior is shown in [15]. Aschemann et al. [1] give a contribution to a flatness-based trajectory control of a pneumatically driven carriage. In [7] instead of static characteristic lines a dynamical model of the muscle is described improving the dynamical behavior of the system.

2 Design

As already mentioned the hexapod consists of a moving platform and a fixed base platform coupled by six fluidic muscles. The muscles run with a maximum pressure of 6 bar delivering forces up to 6000 N/muscle by a weight of 0.2 kg, see Figure 5 for the characteristic lines of the used muscles. The platform in Figure 1 has a height of 0.5 m by a diameter of 0.4 m. The weight is about 20 kg. Due to the construction, friction effects only occur in the ball bearings at the ends of the muscles and are therefore negligible. The muscle itself does not have any friction. The spring applying all compressive forces is from a passenger car with a stiffness in longitudinal direction of about 10^5 N/m. The desired trajectories can either be planned offline, or directly taken from a force feedback joystick with six degrees of freedom, built again as a Stewart platform. A detailed description for this joystick is given in [11].

Fig. 1 Photo of the system. The left side of the photo shows the joystick, while the right side is the pneumatically driven hexapod.

The electrical buildup is shown in Figure 2. All the control schemes are designed by using Matlab/Simulink. With the Real Time Workshop the control code is built for a Real Time Application Interface (RTAI) patched linux kernel, running on an embedded computer board with a 1 GHz processor. Phytec eNET-CAN Boards on the PC104 bus of the embedded system perform the CAN communication (1MBaud) to special designed analog–digital and digital–analog converters. These are directly connected to the joystick and the hexapod. The measured values are the lengths of each actuator by linear potentiometers and the pressure in the muscles. The actuating values are the voltages for the pressure sensitive valves.

3 Kinematics

For the kinematical and the dynamical model of the robot (in Sect. 4) the vector $\mathbf{q} = (x,\ y,\ z,\ \alpha,\ \beta,\ \gamma)^T$ (TCP coordinates) is used comprising the minimal coordinates. x, y, z are the coordinates of the TCP, while α, β, γ is a representation of the orientation in Cardan angles, see Eq. (2) for a definition of the rotation sequence. Figure 3 shows a truncated model of the system. In contrast to serial robots, the inverse kinematics is easy to solve, see [9]. The length of the ith leg m_i is equal to

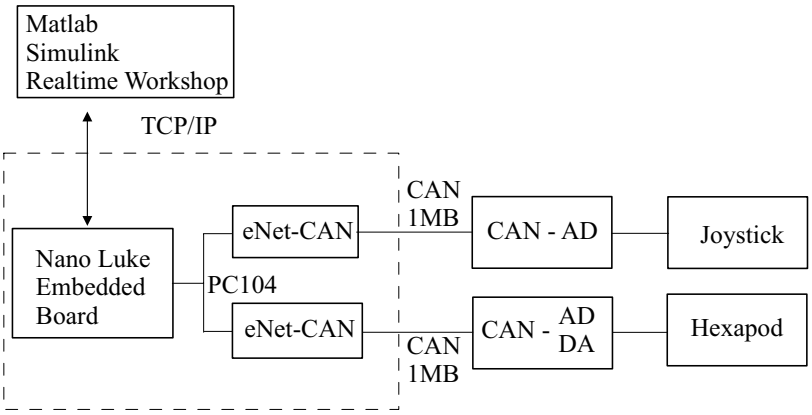

Fig. 2 Signals and electrical design.

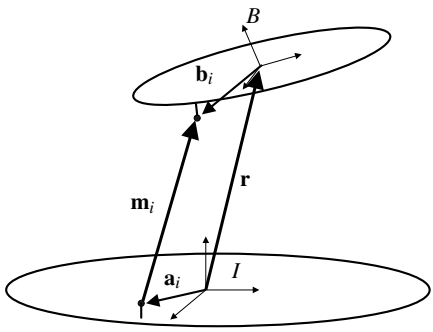

Fig. 3 Topology of a hexapod leg.

$$
\begin{aligned}
{}_I\mathbf{m}_i &= {}_I\mathbf{r} + \mathbf{A}_{IB}\,{}_B\mathbf{b} - {}_I\mathbf{a}_i, \\
m_i &= \sqrt{{}_I\mathbf{m}_i^T\ {}_I\mathbf{m}_i}
\end{aligned}
\tag{1}
$$

with the position $\mathbf{r}$ of the moving plate and the rotation matrix $\mathbf{A}_{IB}$ transforming coordinate system B to system I. By choosing Cardan angles as representation for the orientation for the moving plate, the rotation matrix is

$$
\mathbf{A}_{IB} = \mathbf{A}_{BI}^T = \left(\mathbf{A}_\gamma \mathbf{A}_\beta \mathbf{A}_\alpha\right)^T = \mathbf{A}_\alpha^T \mathbf{A}_\beta^T \mathbf{A}_\gamma^T \tag{2}
$$

where $\mathbf{A}_\alpha$ is an elementary rotation about the x axis, $\mathbf{A}_\beta$ about the y axis and $\mathbf{A}_\gamma$ about z, respectively.

In contrast to the inverse kinematics, the forward kinematics evaluates by given muscle lengths the position and orientation of the TCP. A satisfying analytical solution is not available. There are some approaches in [6] which are not usable in realtime computations. However, in this paper a numerical solution is chosen. A set of constraint equations $\boldsymbol{\phi}$ including the inverse kinematics,

$$
\phi = \left(\phi_1 \ \ldots \ \phi_6\right)^T, \quad \phi_i = m_i|_{\mathbf{q}^{(n)}} - m_{i,d} = 0, \quad i = 1, \ldots, 6,
$$

where $m_{i,d}$ is the desired length of muscle i leads to the Newton–Raphson iteration scheme [3]

$$\mathbf{q}^{(n+1)} = \mathbf{q}^{(n)} - \underbrace{\phi'\big|^{-1}_{\mathbf{q}^{(n)}}\ \phi|_{\mathbf{q}^{(n)}}}_{\delta^{(n)}} \tag{3}$$

with $\mathbf{q}^{(n)}$ the solution of the nth iteration, δ the Newton direction and $\boldsymbol{\phi}' = \partial\boldsymbol{\phi}/\partial\mathbf{q}$ is the appropriate Jacobian. Due to perfect starting points only two iterations per timestep are necessary for an adequate accuracy. To decrease the calculation time for Eq. (3) it is more efficient to evaluate $\boldsymbol{\delta}$ from

$$\phi'\big|_{\mathbf{q}^{(n)}}\,\delta^{(n)} = \phi|_{\mathbf{q}^{(n)}}$$

by solving this systems of equations iteratively, see [5] for details.

4 Dynamics

There are several methods for deriving the equations of motion. In this work, the projection equation – a synthetical method – is used. Linear momentum $\mathbf{p} = m\ \mathbf{v}_c$ and angular momentum $\mathbf{L} = \mathbf{J}\ \boldsymbol{\omega}_c$ are projected into the minimal space (minimal velocities $\dot{\mathbf{q}}$) via the appropriate Jacobians

$$\sum_{i=1}^{N}\left(\left(\frac{\partial_R\mathbf{v}_c}{\partial\dot{\mathbf{q}}}\right)^T\ \left(\frac{\partial_R\boldsymbol{\omega}_c}{\partial\dot{\mathbf{q}}}\right)^T\right)\begin{pmatrix}{}_R\dot{\mathbf{p}} + {}_R\tilde{\boldsymbol{\omega}}_{IR}\,{}_R\mathbf{p} - {}_R\mathbf{f}^e\\ {}_R\dot{\mathbf{L}} + {}_R\tilde{\boldsymbol{\omega}}_{IR}\,{}_R\mathbf{L} - {}_R\mathbf{M}^e\end{pmatrix}_i = \mathbf{Q}.$$

All the values like the translational velocity $\mathbf{v}_c$ or the rotational velocity of the center of gravity $\boldsymbol{\omega}_c$ can be inserted in arbitrary coordinate systems R. In contrast to $\boldsymbol{\omega}_c$, $\boldsymbol{\omega}_{IR}$ is the velocity of the used reference system. The matrix $\mathbf{J}$ is the inertial tensor, while $\tilde{\boldsymbol{\omega}}\,\mathbf{p}$ characterizes the vector product $\boldsymbol{\omega}\times\mathbf{p}$. $\mathbf{f^e}$ and $\mathbf{M^e}$ are imposed forces and moments acting on the ith body.

In the present case a body fixed reference system B is used for the description of the moving plate. The velocities in this system read

$${}_B\omega_c = {}_B\omega_{IB} = \left[\,\mathbf{A}_\gamma\mathbf{A}_\beta\mathbf{e}_1\ \mathbf{A}_\gamma\mathbf{e}_2\ \mathbf{e}_3\,\right]\begin{pmatrix}\dot{\alpha}\\ \dot{\beta}\\ \dot{\gamma}\end{pmatrix},$$

$${}_B\mathbf{v}_c = {}_B\dot{\mathbf{r}}_c + {}_B\tilde{\omega}_{IB}\,{}_B\mathbf{r}_c.$$

The weight of the muscles is about dimensions smaller than the moving plate and load, so it can be neglected. Special investigations have to be performed in the modeling of the muscles and the spring forces. The principle of virtual work reads

$$\delta W = \delta\mathbf{q}^T\mathbf{Q} = \sum\delta\,{}_I\mathbf{r}_i^T\,{}_I\mathbf{F}_i = \sum\delta\mathbf{q}^T\left(\frac{\partial_I\mathbf{r}_i}{\partial\mathbf{q}}\right)^T{}_I\mathbf{F}_i$$

with

$$ {}_I\mathbf{F}_i = F_i \frac{{}_I\mathbf{m}_i}{\| {}_I\mathbf{m}_i \|}. $$

F_i is the force of the ith muscle, while ${}_I\mathbf{m}_i / \| {}_I\mathbf{m}_i \|$ is the normalized direction, see Eq. (1). The spring for the compressive forces is included with the help of a potential $\mathbf{Q} = -(\partial V / \partial \mathbf{q})^T$, where the potential function V can be approximated by

$$ V = \frac{1}{2} c_{\text{trans},z} (z - l_0)^2 + \frac{1}{2} c_{\text{trans},xy} (x^2 + y^2 + \frac{1}{2} c_{\text{rot},\gamma} \gamma^2 + \frac{1}{2} c_{\text{rot},\alpha\beta} (\alpha^2 + \beta^2). $$

As can be seen in the potential function, there is a different stiffness in z ($c_{\text{trans},z}$) and x, y ($c_{\text{trans},xy}$) direction and in γ ($c_{\text{rot},\gamma}$) and α, β ($c_{\text{rot},\alpha\beta}$) direction. The values are evaluated by an identification process. l_0 is the length of the force free spring. The dynamical modeling process delivers the equations of motion in the form

$$ \mathbf{M}(\mathbf{q})\, \ddot{\mathbf{q}} + \mathbf{g}(\mathbf{q}, \dot{\mathbf{q}}) = \mathbf{B}(\mathbf{q})\mathbf{u}, \tag{4} $$

where $\mathbf{u} = (F_1 \ldots F_6)^T$ is the control input of the six muscle forces. $\mathbf{M}(\mathbf{q})$ is the mass matrix and $\mathbf{g}(\mathbf{q}, \dot{\mathbf{q}})$ contains all nonlinear effects like coriolis forces, gravitational forces and so on. To calculate the inverse dynamical model the equation of motion is solved for the forces $\mathbf{u}$ by premultiplying Eq. (4) with $\mathbf{B}^{-1}$. Due to the mechanical design, a singular position of the hexapod and therefore a singular matrix $\mathbf{B}$ is not possible.

5 Control

To test the performance of the robot on a test rig, an embedded system, running with a RTAI patched Linux kernel, is used to achieve the real time performance. A Nano Luke Board equipped with a 1 GHz processor fulfills the requirements to let all computations run in a sample time of 2 milliseconds. Matlab/Simulink is used to develop the overall software system whereas the computationally intensive functions are included as C code. Figure 4 shows the control concept in a schematic way for one leg.

The desired values in TCP coordinates can either be generated by a trajectory generator (offline) or by a joystick (online). The offline paths are needed for manipulation tasks, while the online ones are useful in the field of fitness where a trainer plans the motion. The TCP coordinates are via the inverse kinematics transformed to the desired lengths and a desired stroke h in % for each muscle is calculated,

$$ h_{d,i} = \frac{m_{d,i}}{m_0} 100\% $$

($m_0 \ldots$ total length of the muscles). A PID controller delivers in combination with the inverse dynamic model

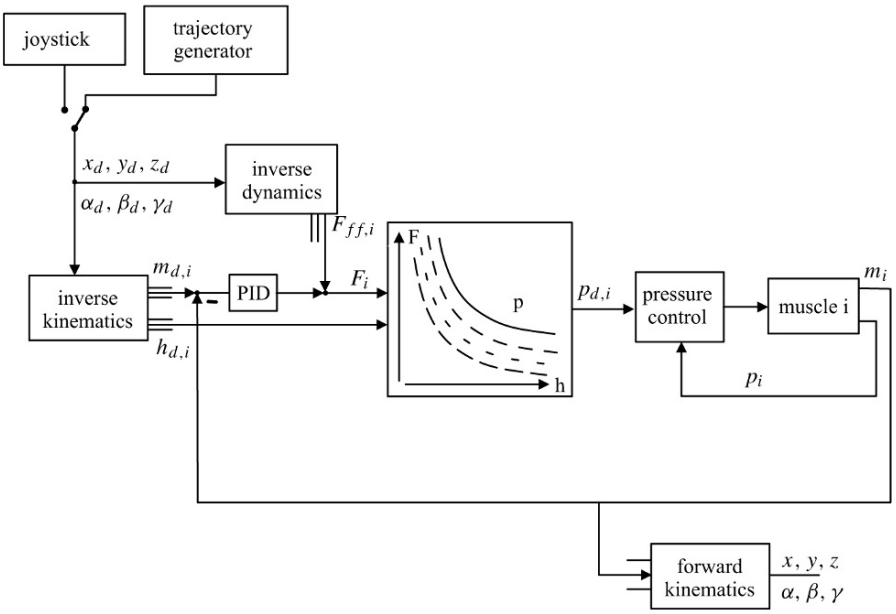

Fig. 4 Control concept.

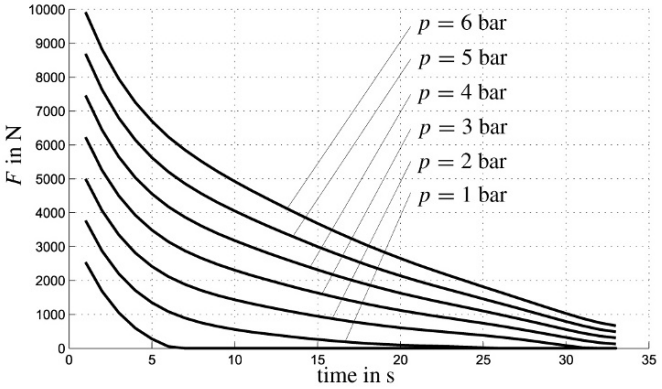

Fig. 5 Characteristic lines of a fluidic Festo muscle DMSP40.

$$\mathbf{F}_{ff} = \mathbf{B}(\mathbf{q}_d)^{-1}(\mathbf{M}(\mathbf{q}_d)\ddot{\mathbf{q}}_d + \mathbf{g}(\mathbf{q}_d, \dot{\mathbf{q}}_d))$$

the needed muscle force. The force–pressure–stroke relation of the muscles is represented by characteristic lines, see Figure 5, which can be approximated by a look up table to fulfill the requirement of low computational effort. The lines in Figure 5 are identified in a statical experimental process.

Assuming an input force F_i and the stroke $h_{d,i}$, the desired pressure $p_{d,i}$ is obtained as a direct result of this relation. A succeeding PID controller tracks the

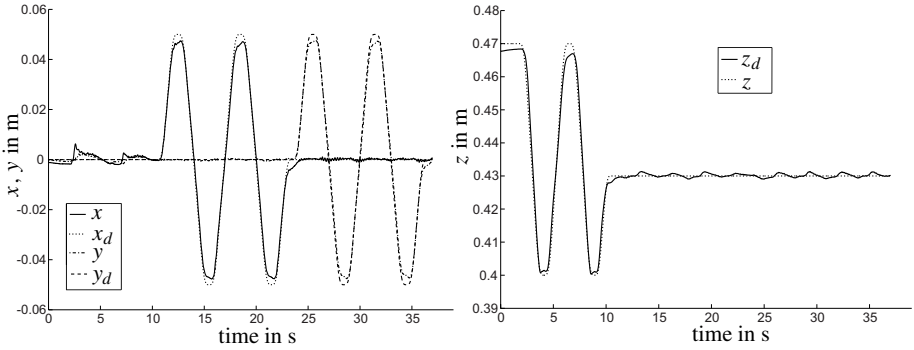

Fig. 6 Measured and desired TCP coordinates.

Fig. 7 Measured and desired length of muscle 1.

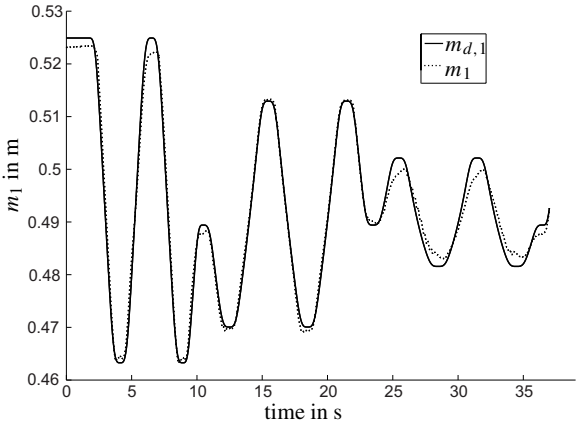

pressure of the ith muscle. The system is tested with desired trajectories shown in Figure 6. The maneuver is a fast movement in z-direction, followed by x and y movements for the TCP. There is a small control error due to limitations in the input variables of the pneumatic valves.

Figure 7 exemplarily shows the desired ($m_{d,1}$) and the measured (m_1) length of muscle 1. The behavior is satisfactory with respect to the required accuracy. The pressure control behavior for muscle 1 is shown in Figure 8.

6 Conclusions

In this paper we presented a new type of parallel mechanism using fluidic muscles as an innovative driving system. A main advantage is the simple design of the Stewart platform consisting of a moving plate, a fixed plate connected by six muscles and a pre-stressed spring. The six degrees of freedom ($x, y, z, \alpha, \beta, \gamma$) are interrelated to

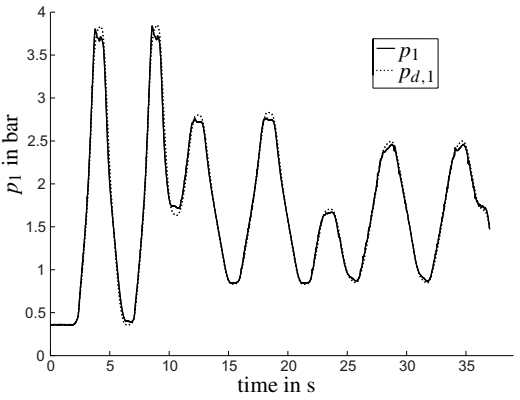

Fig. 8 Measured and desired pressure of muscle 1.

the lengths of the muscles $(m_1, \ldots, m_6)$ by kinematical computations. The inverse kinematical problem is easily solved by vector chains, while the forward kinematics is evaluated by a Newton iteration scheme. From a dynamical point of view, the system consists of nine bodies. A representation in minimal space, where constraint forces are faded out, is evaluated by the Projection Equation leading to a simulation model and an inverse dynamical model enhancing the control performance. Due to the high nonlinearities of the pneumatic muscles, a lot of work has to be done in the evaluation of the control concept. The shown cascaded scheme consisting of pressure control, linearization, model based feed forward control leads to a satisfying behavior. In the future investigations, observers to model the load (mass, center of gravity) have to be implemented.

Acknowledgements The authors gratefully acknowledge our industrial partner FerRobotics Compliant Robot Technology GmbH for their support during this project and the perfect co-operation.

References

1. Aschemann, H., Hofer, E.: Flatnessbased control of a carriage driven by pneumatic muscles. In *Proceedings of MMAR*, pp. 1219–1224 (2003).
2. Bremer, H.: *Dynamik und Regelung mechanischer Systeme*. Teubner Studienbücher, Stuttgart (1988).
3. Eich-Soellner, E., Führer, C.: *Numerical Methods in Multibody Dynamics*. Teubner, Stuttgart (1998).
4. Föllinger, O.: *Regelungstechnik – Einführung in die Methoden und ihre Anwendungen*. Hüthig Buch Verlag Heidelberg, Heidelberg (1996).
5. Hoffmann, A., Marx, B., Vogt, W.: *Mathematik für Ingenieure 1*. Pearson, München (2005).
6. Husty, M.: An algorithm for solving the direct kinematics of general stewart-gough platforms. *Mechanism and Maschine Theory* **31**(4), 365–379 (1996).
7. Kerscher, T., Albiez, J., Zöllner, J., Dillmann, R.: Evaluation of the dynamic model of fluidic muscles using quick-release. First IEEE/RAS-EMBS International Conference on Biomedical Robotics and Biomechatronics (2006).

8. Khalil, W., Dombre, E.: *Modeling, Identification and Control of Robots*. Kogan Page Science, London (2004).
9. Merlet, J.: *Parallel Robots*. Kluwer Academic Publishers, Dordrecht (2000).
10. Neumann, R., Bretz, C., Volzer, J.: Ein Positionierantrieb mit hoher Kraft: Positions- und Druckregelung eines künstlichen pneumatischen Muskels. 4. International Fluidtechnik Kolloquium (2004).
11. Ollmann, H.: *Modellierung, Konstruktion und Regelung einer 6-DOF Stewart Plattform*. JK University Linz, Linz (2006).
12. Riebe, S.: *Aktive Schwingungsisolierung und Bahnregelung von Hexapodsystemen*. VDI Verlag, Düsseldorf (2005).
13. Riebe, S., Ulbrich, H.: Stabilization and tracking control of a parallel kinematic with six degrees-of-freedom. 5th EUROMECH Solid Mechanics Conference (ESMC) (2003).
14. Schwandtner, J.: *Konstruktion, Modellierung und Regelung eines Hexapods mit Luftmuskel Aktuatorik*. JK University Linz, Linz (2007).
15. Singh, M.D., Liem, K., Kecskemethy, A., Neumann, R.: Design and control of a pneumatic hybrid actuator. In *PAMM Proceedings for Applied Mathematics and Mechanics*, pp. 497–498 (2005).
16. Singh, M.D., Liem, K., Neumann, R., Kecskemethy, A.: Modeling of a pneumatic hybrid actuator using an exponential approach for approximation of the valve-actuator behaviour. In *PAMM Proceedings for Applied Mathematics and Mechanics*, pp. 803–804 (2006).